




Excimer laser-assisted corneal epithelial pattern ablation for corneal cross-linking

Jurriaan Brekelmans,^{1,2}  Mor M. Dickman,¹  Shwetabh Verma,^{3,4,5,6} Samuel Arba-Mosquera,³ Ruth Goldschmidt,² Alexandra Goz,^{2,7} Alexander Brandis,⁸ Tos T.J.M. Berendschot,¹  Isabelle E.Y. Saelens,¹ Arie L. Marcovich,^{2,7} Avigdor Scherz² and Rudy M.M.A. Nuijts¹

¹University Eye Clinic Maastricht, Maastricht University Medical Center, Maastricht, the Netherlands

²Department of Plant Science and Environmental Health, the Weizmann Institute of Science, Rehovot, Israel

³Department of Research and Development, SCHWIND Eye-Tech-Solutions, Kleinostheim, Germany

⁴Experimental Radiation Oncology, University Medical Center Mannheim, Heidelberg, Germany

⁵Interdisciplinary Center for Scientific Computing (IWR), Heidelberg University, Heidelberg, Germany

⁶Central Institute for Computer Engineering (ZITI), Heidelberg University, Heidelberg, Germany

⁷Department of Ophthalmology, Kaplan Medical Center, Rehovot, Israel

⁸Department of Biological Services, the Weizmann Institute of Science, Rehovot, Israel

ABSTRACT.

Purpose: To determine corneal cross-linking (CXL) efficacy and chromophore penetration after excimer laser-assisted patterned de-epithelialization.

Methods: Two-hundred-twenty porcine eyes were de-epithelialized *ex vivo*, either fully (mechanical; $n = 88$) or patterned (excimer laser; $n = 132$). Consecutively, corneas were impregnated with hypo- or hyperosmolar riboflavin (RF; $n = 20$, RF-D; $n = 40$, respectively) or water-soluble taurine (WST11; $n = 40$, and WST-D; $n = 40$, respectively), or kept unimpregnated ($n = 80$). Sixty corneas were subsequently irradiated, inducing CXL, with paired contralateral eyes serving as controls. Outcome measurements included strip extensimetry to assess CXL efficacy, and spectrophotometry and fluorescence microscopy to determine stromal chromophore penetration.

Results: All tested chromophores induced significant CXL ($p < 0.001$), ranging from 7.6% to 14.6%, with similar stiffening for all formulations ($p = 0.60$) and both de-epithelialization methods ($p = 0.56$). Light transmittance was significantly lower ($p < 0.001$) after full compared with patterned de-epithelialization. Stromal chromophore penetration was comparable between fully and patterned de-epithelialized samples, with full penetration in RD and RF-D samples and penetration depths measuring $591.7 \pm 42.8 \mu\text{m}$ and $592.9 \pm 63.5 \mu\text{m}$ for WST11 ($p = 0.963$) and $504.2 \pm 43.2 \mu\text{m}$ and $488.8 \pm 93.1 \mu\text{m}$ for WST-D ($p = 0.669$), respectively.

Conclusions: Excimer laser-assisted patterned de-epithelialization allows for effective CXL. Stromal chromophore concentration is, however, reduced, which may have safety implications given the need for sufficient UVA attenuation in RF/UVA CXL. The different safety profile of near-infrared (NIR) may allow safe WST11/NIR CXL even with reduced stromal chromophore concentration values. *In vivo* studies are needed to evaluate the benefits and further assess safety of excimer laser-assisted patterned de-epithelialization for corneal CXL.

Key words: corneal cross-linking – WST11 – riboflavin – excimer laser

Acta Ophthalmol. 2022; 100: 422–430

© 2021 The Authors. Acta Ophthalmologica published by John Wiley & Sons Ltd on behalf of Acta Ophthalmologica Scandinavica Foundation.

This is an open access article under the terms of the Creative Commons Attribution-NonCommercial-NoDerivs License, which permits use and distribution in any medium, provided the original work is properly cited, the use is non-commercial and no modifications or adaptations are made.

doi: 10.1111/aos.15021

Introduction

Corneal collagen cross-linking (CXL) is applied to arrest thinning and destabilization associated with keratoconus (KC) progression. CXL using riboflavin (RF) and ultraviolet A (UVA) light is currently the only clinically approved treatment modality. Although good clinical results showing stabilization of disease for up to 10 years, the procedure has several downsides (O'Brart et al. 2015; Poli et al. 2015; Raiskup et al. 2015). One major disadvantage is related to epithelial debridement, which is associated with discomfort and postoperative complications, such as haze formation, delayed healing and infection (Koller, Mrochen & Seiler 2009; Cagil et al. 2015; Maharana et al. 2018). Various approaches have been suggested to overcome the need for full epithelial debridement, including epithelium-on cross-linking, chemical modification of Riboflavin and mechanical removal of only part of the epithelium (Rechichi et al. 2013; Razmjoo et al. 2014; Hashemi et al. 2015; Galvis et al. 2016; Stulting et al. 2018). Thus far, most reports show reduced RF penetration and reduced efficacy for epithelium-on procedures (Lombardo et al. 2015; Akbar et al. 2017; Godefrooij et al. 2017).

Besides RF/UVA CXL, several other light-activated chromophores have been investigated, providing corneal stiffening

with different drug and treatment characteristics (Marcovich et al. 2012; Cherfan et al. 2013; Alageel et al. 2018). One alternative is water-soluble taurine (WST11) (Marcovich et al. 2012). In contrast to RF, which uses potentially toxic UVA light, WST11 can be activated by near-infrared (NIR) light at 755 nm, which is safe to the eye at intensities beyond what is needed for effective CXL (ICNIRP (International Commission on Non-ionizing Radiation Protection) (1997)). Due to their different characteristics, both chromophores rely on different stromal diffusion patterns to assure safety. Alternative CXL modalities offer a perspective to patients non-responsive to or unsuitable for RF/UVA CXL, such as patients with thin corneas.

In this study, we use a clinically approved excimer laser platform to selectively ablate the corneal epithelium in a patterned fashion, creating 350 μm wide and 375 μm spaced epithelial channels to allow for chromophore diffusion while leaving up to 60% of the epithelium in the treated area in situ. We hypothesize this may promote faster epithelial healing, reduce patient discomfort and increase treatment safety. In an *ex vivo* porcine model, we evaluated stromal penetration, light attenuation and biomechanical stiffening of the two chromophores WST11 and RF, in hypo- and hyperosmotic formulations, after full mechanical or patterned excimer laser-assisted de-epithelialization.

Materials and Methods

Sample preparation

Ex vivo porcine model

We included 220 paired porcine eyes, freshly obtained from a local abattoir and macroscopically inspected for damage, haze, oedema or surface irregularities. Porcine corneas provide a well-established *ex vivo* animal model for preclinical research on corneal procedures, with reported central corneal thickness (CCT) *ex vivo* of approximately 920 μm, shown to remain stable for up to 24 hr after enucleation (Jay et al. 2008; Nibourg & Koopmans 2014; Stoddard et al. 2018).

Manual and excimer laser-assisted de-epithelialization

All 220 corneas were de-epithelialized, either manually ($n = 88$) or excimer

laser-assisted ($n = 132$). Full manual de-epithelialization of the central epithelium with a 9 mm diameter was performed using a blunt hockey knife, following the Dresden protocol (Wollensak, Spoerl & Seiler 2003), similar to clinical practice without the application of alcohol. Selective patterned de-epithelialization was performed over the central 9 mm using the SCHWIND Amaris excimer laser (SCHWIND Eye-Tech-Solutions, Kleinostheim, Germany). Epithelial channels with a radius of 350 μm, the minimal radius possible for this excimer laser apparatus, were created in a hexagonal pattern with equal distance between channels (Fig. 1, Fig. 2, supplementary Figure S1). Pilot studies showed chromophore diffusion became heterogenous if the spacing between channels was greater than

375 μm. Thus, the distance between channels was set at 375 μm, resulting in approximately 40% total surface ablation of the treated area (Supplementary equation S1). Ablation depth was determined for each cornea individually and set to penetrate the full epithelial thickness, measured by ocular coherence tomography (OCT), as described below.

Chromophore preparation

Four different formulations of photosensitizer were prepared: RF, RF with 20% Dextran T500 (RF-D), WST11 and WST11 with 20% Dextran T500 (WST-D). RF solutions (Sigma-Aldrich, St. Louis, Missouri, USA) were prepared at a concentration of 0.1%, WST11 (Steba Laboratories Ltd., Rehovot, Israel) solutions at

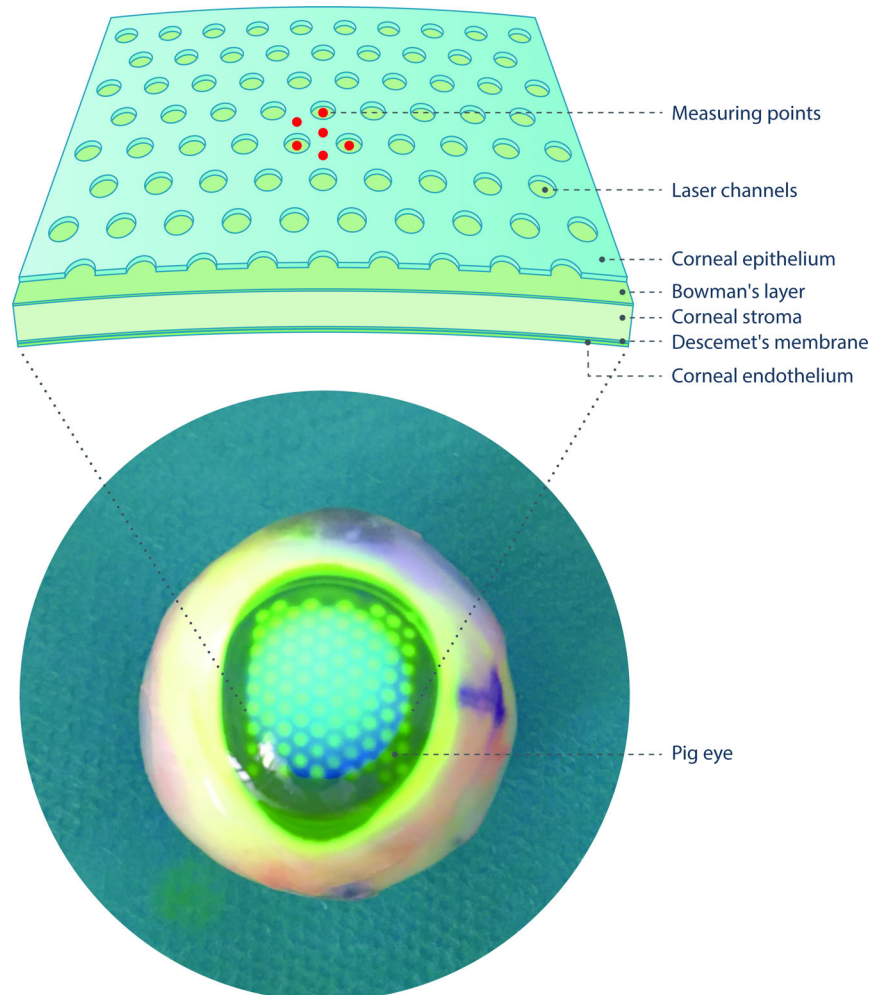


Fig. 1. F Porcine cornea, after excimer laser-patterned de-epithelialization and riboflavin (RF) impregnation (bottom), and schematic representation of hexagonal pattern of ablated epithelium (top). Radius of the channels measured 350 μm, with a distance between the channels of 375 μm. This corresponds to approximately 60% of the epithelium remaining (following Supplementary equation S1). Fluorescence was imaged focally in three, centred at an epithelial channel or at unablated epithelium (red marks).

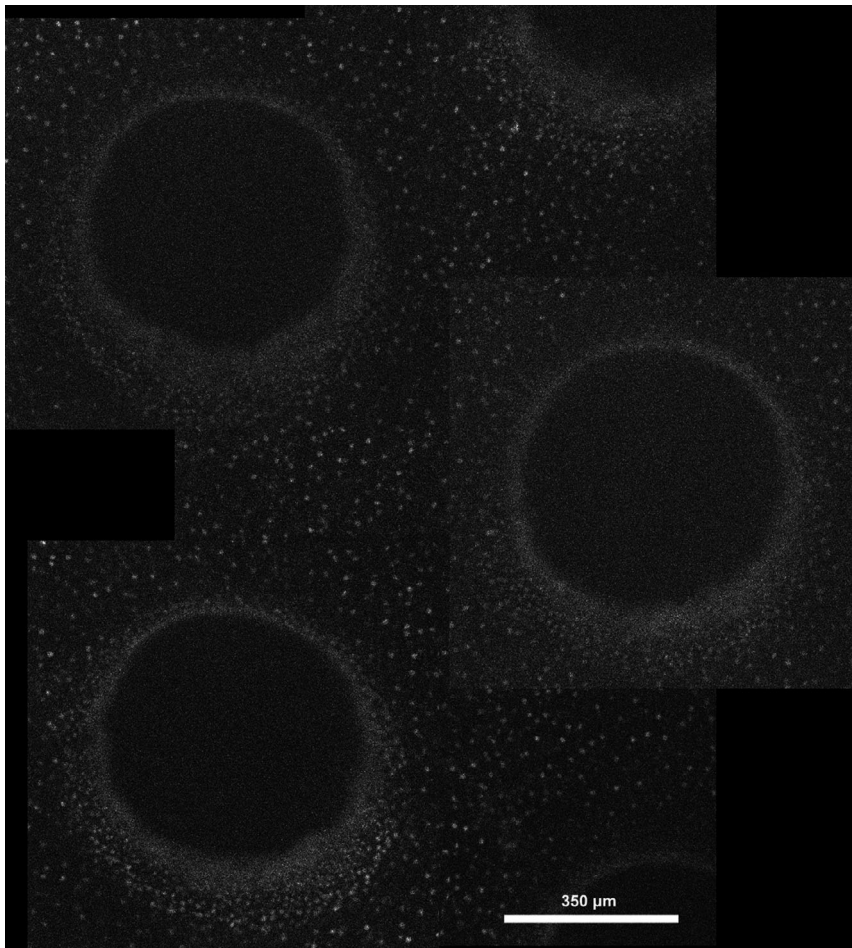


Fig. 2. Stitched image derived by fluorescence microscopy showing several epithelial channels, and intermediate remaining epithelium, with cell nuclei stained by propidium iodine.

2.5%. All solutions were prepared in saline and corrected to a pH between 7.2 and 7.3.

Sample allocation

Samples were divided into two groups: 100 eyes were used to assess safety (i.e. stromal chromophore diffusion; Fig. 3A) and 120 eyes were used to determine CXL efficacy (Fig. 3B). In the first group (i.e. safety group), allocation of paired eyes to each chromophore was done in a layered design (Supplementary Table S1). In the second group (i.e. efficacy group), a paired setup was used with one eye of each pair receiving full CXL treatment, with the contralateral eye serving as control (de-epithelialized only).

Sample treatment

After de-epithelialization, a self-manufactured plastic well, 12 mm in diameter with round edges, was placed

on top of corneas allocated to receive chromophore impregnation. The well was filled with 1 mL of the respective photosensitizer, providing a constant supply of chromophore, alike the chromophore film existing during frequent topical chromophore application (Wollensak et al. 2010). Control corneas were left unimpregnated. After 30 or 20 min of impregnation, for RF and RF-D, and WST and WST-D, respectively, the remaining photosensitizer was removed and the cornea was briefly rinsed with 2 mL of distilled water to remove excess photosensitizer.

In addition to the above, in the CXL efficacy group, 60 eyes of 60 pairs received additional irradiation treatment to achieve full CXL treatment (Fig. 3B). CXL efficacy was assessed for RF-D, WST11 and WST-D-based CXL. After either RF-D or WST11/WST-D impregnation, corneas were irradiated for 30 min by either UVA light of 365 nm at 3 mW/cm² (SCHWIND CXL-365 vario system; SCHWIND Eye-Tech-

Solutions, Kleinostheim, Germany) or NIR light of 753 nm at 10 mW/cm² (Cerelas PDT 753, CeramOptec GmbH, Bonn, Germany), respectively. During irradiation, every 5 min, a drop of distilled water was placed on the cornea to prevent dehydration.

Sample evaluation

Central corneal and epithelial thickness measurements

Corneas were imaged with a CASIA2 OCT (Tomey, Nagoya, Japan), prior to (patterned) de-epithelialization, directly after de-epithelialization and, when applicable, after photosensitizer impregnation and after irradiation (Fig. 4). Central epithelial thickness (CET) was determined for each cornea individually. Following mechanical de-epithelialization, CET was determined by calculating the difference between CCT prior and directly after de-epithelialization. In the excimer laser ablation group, the residual epithelium did not allow similar subtraction, and thus, CET was determined by averaging five manual CET measurements in the central four millimetres of the pre-excimer laser ablation high-resolution OCT image.

Safety

Described in detail below, treatment safety was assessed by absorbance spectrophotometry (*total* indicating stromal chromophore concentration and *direct* determining the de-epithelialization's scattering effect) and confocal fluorescence microscopy (imaging stromal chromophore penetration depth).

Absorbance spectrophotometry

Corneas in the chromophore diffusion group (*n* = 100, Fig. 3A) were consecutively placed in the beam of two UV-visible spectrophotometers: adapted with an integrative sphere (V-570, Jasco Inc., Mary's Court, MD, USA) or without (Evolution 220, Thermo Fischer Scientific Inc., Waltham, MA, USA). *Total* and *direct* absorbance was measured between 300 and 900 nm with a spectral bandwidth of 5 nm. *Total* spectroscopy, measuring all transmitted light independent of scattering, was used to assess stromal chromophore concentration in the five subgroups (native/RF/RF-D/WST11/WST-D impregnated). Given the toxic nature of UVA light, sufficient stromal chromophore is needed to attenuate the UVA light. Stromal

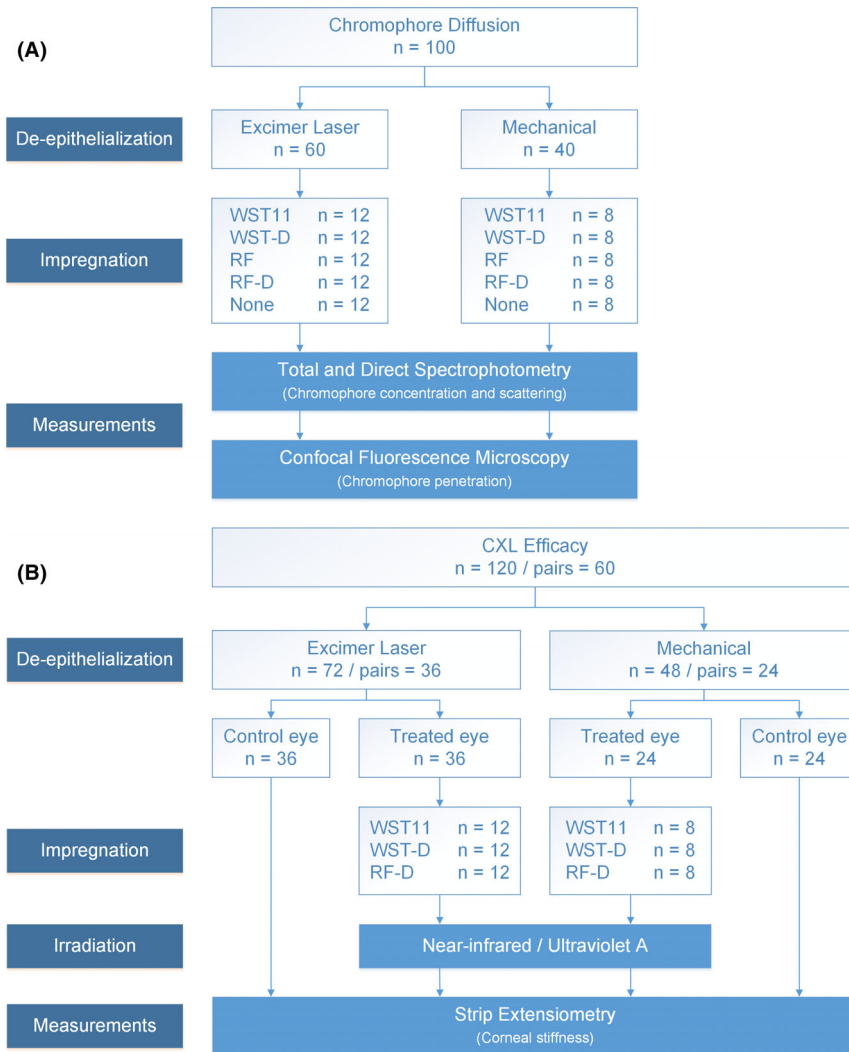


Fig. 3. Study flowchart of cornea allocated to assess chromophore diffusion and penetration (A) and corneal cross-linking (CXL) efficacy (B).

chromophore concentration serves as an indirect measure for treatment safety. *Direct* spectroscopy, excluding scattered light, was used to assess changes in transmittance induced by excimer laser ablation. A curve was fitted including a wavelength-dependent (Rayleigh) and wavelength-independent factors (Tryptophan; derived from Van de Kraats et al.) (van de Kraats & van Norren 2007). The percentual decrease for both factors was calculated as a measure of changes in the cornea’s optical properties.

Confocal fluorescence microscopy

After absorbance spectrophotometry, corneal chromophore diffusion was assessed using an inverted confocal fluorescence microscope (BX61 Olympus, Tokyo, Japan), with images taken at 10 μm steps using a CCD camera (Cascade 512B, Roper Sci., New Jersey,

USA). Samples were stained by 5 μM propidium iodide (PI), allowing visualization of the sample’s stromal borders. All samples were excited at 561 nm with fluorescence being recorded at 617 nm to image PI-stained cell nuclei. Additionally, samples were consecutively excited at 488 nm (RF-based impregnated corneas) or 755 nm (WST11-based impregnated corneas), or at both 488 nm and 755 nm (unimpregnated control corneas). Fluorescence intensity was recorded above 525 nm and 760 nm using a filter, for RF and WST respectively. Per cornea, above-mentioned images were taken at three (mechanically de-epithelialized samples) or six (excimer laser-assisted de-epithelialized samples) different areas. In the latter, three areas each were taken, manually centred at either an epithelial channel or a non-ablated area

(Fig. 1). Samples were measured from endothelium to epithelium, to avoid the influence of photobleaching and clear imaging of the chromophore’s penetration front depth. Per image, the intensity in the central 100x100 pixels for both measured channels was averaged and plotted against the depth into the sample, using MATLAB (MATLAB R2018b; The MathWorks Inc., Natick, USA). The stromal border’s position, visualized by the PI staining, was used to determine each frame’s depth within that specific corneal sample. Intensity plots corresponding to RF and WST11 were baseline corrected. Penetration depth was determined to be the point where the intensity dropped below a predetermined threshold value of 30 A.U., below which the signal was considered noise. Supplemental Figure S2 shows a representative example of the output generated by above-mentioned method of a RF impregnated cornea after excimer laser ablation. Per cornea in the excimer laser-assisted group six such graphs were generated (following the sampled areas as shown in figure 1), with three areas sampled in the manual de-epithelialization group.

Efficacy

Treatment efficacy was measured by measuring the sample’s increased stiffness after treatment by strip extensimetry.

Strip extensimetry

In 60 pairs, one eye received full CXL treatment by RF-D, WST11 or WST-D, with the contralateral eye only undergoing similar de-epithelialization as the paired treated cornea (Fig. 3 B). Two 2-mm wide adjacent central strips were cut in superior–inferior direction, and the sample’s Youngs modulus was determined as described previously (Brekelmans et al. 2017). Strips were centred and mounted in the clamps of an extensometer with a 5 kN load cell (Instron 5965; Instron, Norwood, MA, USA) set 6 mm apart, to include treated tissue only. The average of both strips per cornea was used for analysis.

Statistical analysis

Corneal pachymetry and chromophore penetration depth were analysed using analysis of variance (ANOVA), while a repeated-measures ANOVA was used

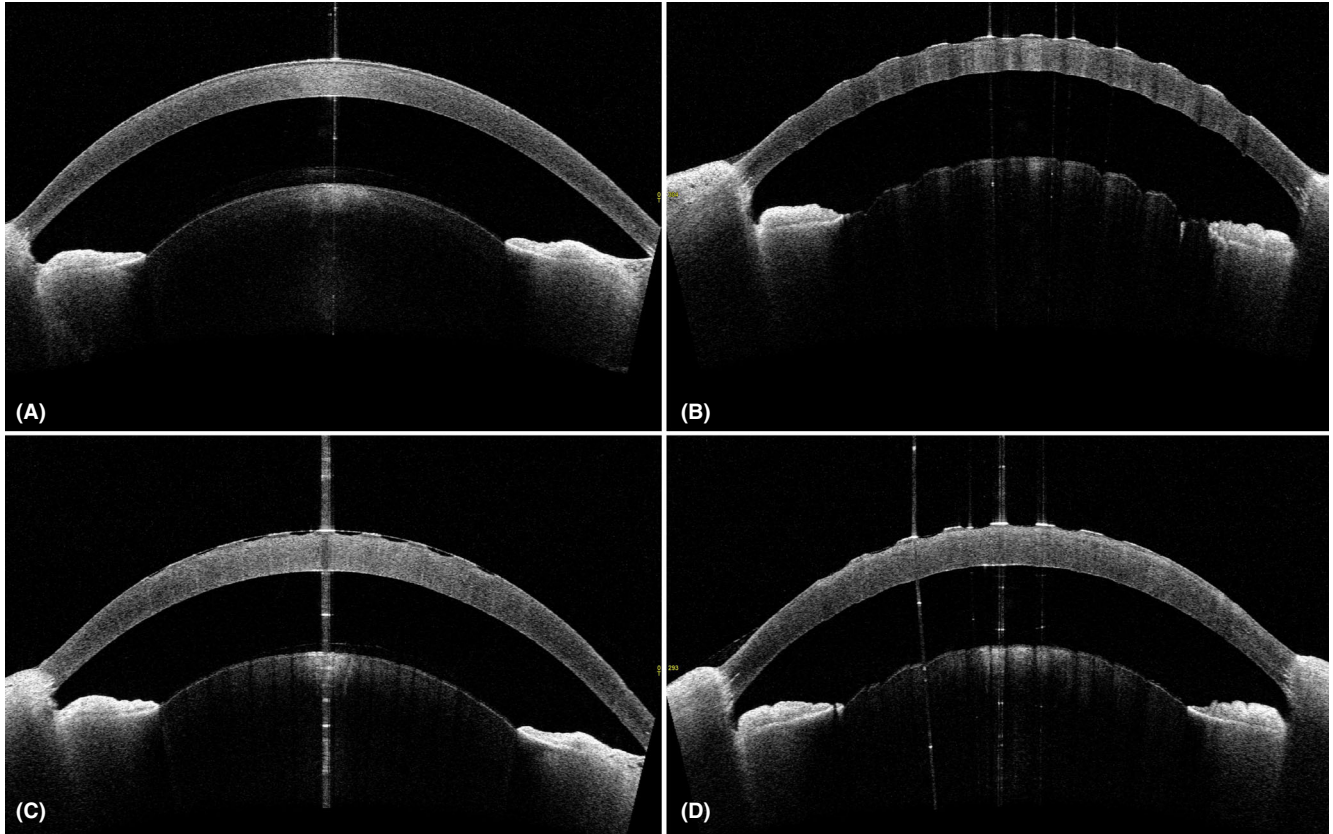


Fig. 4. Ocular coherence tomography images of a porcine cornea, consecutively: (A) prior to procedure, (B) after excimer laser-assisted patterned de-epithelialization, (C) after water-soluble taurine (WST11) impregnation for 20 min, and (D) after near-infrared irradiation for 30 min.

for strip extensometry analysis, permitted by the paired study design. A linear regression model was used for the spectrometry data. Statistical calculations were done with SPSS statistical software (version 23; IBM Corp., Armonk, USA).

Results

Baseline measurements

Central corneal and epithelial thickness

Mean CCT prior to treatment read $919 \pm 69 \mu\text{m}$ ($n = 20$), $927 \pm 103 \mu\text{m}$ ($n = 20$), $919 \pm 81 \mu\text{m}$ ($n = 60$), $893 \pm 64 \mu\text{m}$ ($n = 60$) and $925 \pm 75 \mu\text{m}$ ($n = 60$), for corneas receiving no impregnation, RF, RF-D, WST11 or WST-D impregnation, respectively ($p = 0.147$). Epithelial thickness measured $77 \pm 21 \mu\text{m}$ ($n = 20$), $83 \pm 16 \mu\text{m}$ ($n = 20$), $74 \pm 18 \mu\text{m}$ ($n = 60$), $79 \pm 16 \mu\text{m}$ ($n = 60$) and $75 \pm 20 \mu\text{m}$ ($n = 60$) ($p = 0.212$). Figure 4 shows representative consecutive OCT imaging of a porcine cornea at all stages of sample preparation.

Safety

Absorbance spectrophotometry

Mean total transmittance at 365 nm for RF and RF-D, at 755 nm for WST11 and WST-D impregnated samples, and at both 365 nm and 755 nm for unimpregnated samples is shown in Figure 5. Total transmittance measurements (RF-based at 365 nm, WST11-based at 755 nm) for fully and patterned de-epithelialized corneas read $14.4 \pm 3.2\%$ ($n = 8$) vs. $31.1 \pm 6.7\%$ ($n = 12$), $47.4 \pm 6.9\%$ ($n = 8$) vs. $48.7 \pm 5.5\%$ ($n = 12$), $0.1 \pm 0.0\%$ ($n = 8$) vs. $2.7 \pm 1.0\%$ ($n = 12$) and $4.7 \pm 0.8\%$ ($n = 8$) vs. $17.7 \pm 4.4\%$ ($n = 12$), for RF, RF-D, WST11 and WST-D, respectively. For unimpregnated corneas, total transmittance measured $76.8 \pm 10.8\%$ ($n = 8$) vs. $65.5 \pm 5.3\%$ ($n = 12$) and $93.2 \pm 6.9\%$ ($n = 8$) vs. $90.0 \pm 3.8\%$ ($n = 12$) for fully and patterned de-epithelialized corneas at 365 nm and 755 nm, respectively. In chromophore impregnated corneas (RF, RF-D, WST11 and WST-D), total transmittance was significantly lower in fully de-epithelialized corneas compared with the

patterned de-epithelialized corneas ($p < 0.001$). Compared with hypotonic solutions (RF and WST11), the addition of 20% Dextran (RF-D, WST-D) significantly increased the total transmittance ($p < 0.001$). In native corneas, total transmittance was not significantly different between fully and patterned de-epithelialized corneas ($p = 0.189$).

Direct transmission spectrometry showed reduced transmission after excimer laser-patterned de-epithelialization, compared with full mechanical de-epithelialization. Figure 6 shows the average measured direct transmission of unimpregnated samples, with curve fittings as described in the methods section. Wavelength independent and dependent (Rayleigh scattering) scattering increased by 125% and 77%, respectively, indicating reduced optical clarity by excimer laser-assisted de-epithelialization alone.

Confocal fluorescence microscopy

In unimpregnated corneas, no chromophore fluorescence was detected in either full or patterned de-

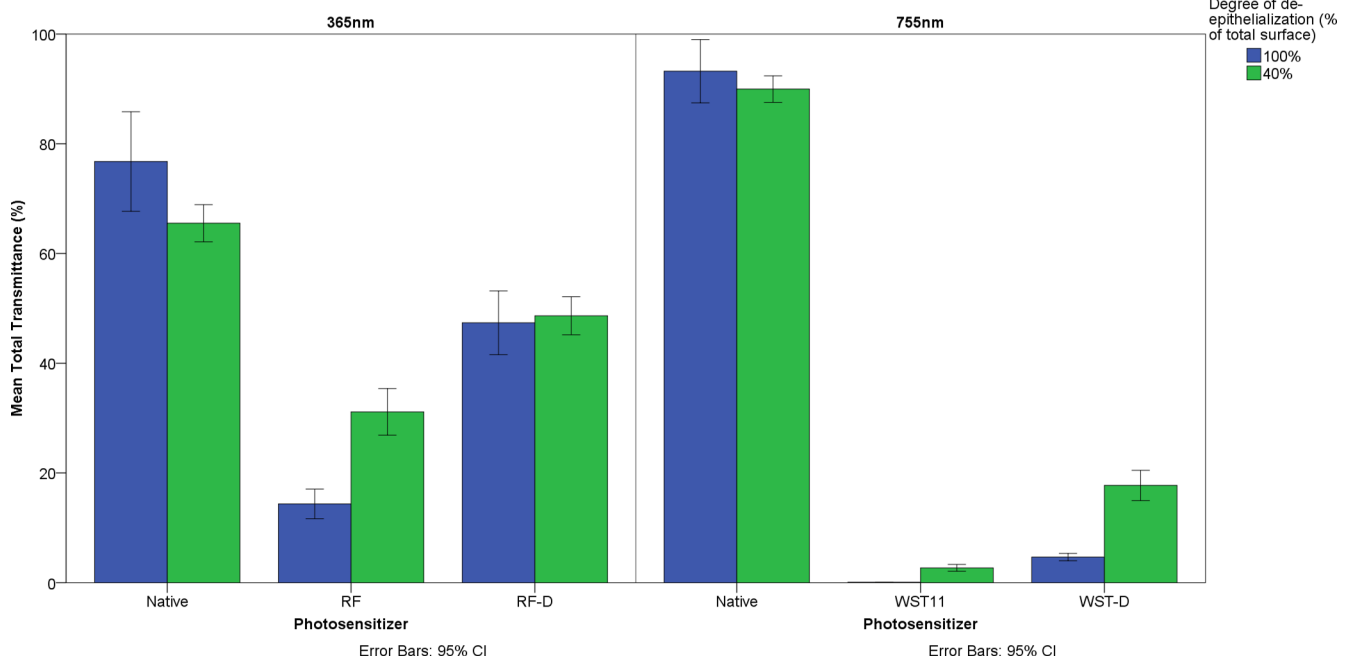


Fig. 5. Mean *total* transmittance of light at 365 nm and 755 nm through porcine cornea, non-impregnated or impregnated with either of four chromophore formulations, after full ($n = 8$ per group) or patterned ($n = 12$ per group) de-epithelialization. Measured applying an integrated sphere. Transmission was significantly higher in patterned de-epithelialized corneas ($p < 0.001$) and in Dextran-enriched (RF-D and WST-D) formulations ($p < 0.001$), indicating lower total stromal chromophore concentrations. Error bars represent 95% confidence interval.

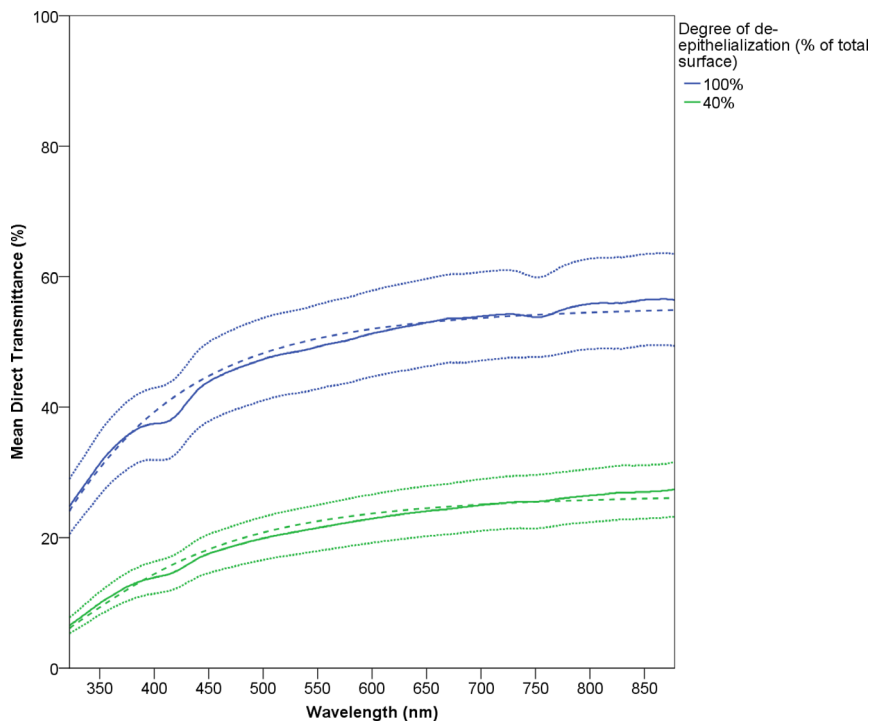


Fig. 6. Mean *direct* transmittance of unimpregnated porcine corneas, fully mechanically de-epithelialized (100%, $n = 8$) or excimer laser-assisted patterned de-epithelialized (40%, $n = 12$). An overall reduced transmittance is seen after patterned de-epithelialization, which we hypothesize may be in part due to the irregular surface created. Dotted lines represent respective 95% confidence intervals of the means, and striped lines indicate best fitted curve.

epithelialization groups. In the RF and RF-D subgroup, full chromophore penetration, regardless of full or patterned

de-epithelialization was seen. In WST11 and WST-D impregnated samples, a clear chromophore penetration front was

noted, with only partial stromal chromophore penetration. When comparing penetration depth in fully and patterned de-epithelialized corneas, no difference was seen for both WST11 ($592 \pm 43 \mu\text{m}$ vs. $593 \pm 64 \mu\text{m}$, $p = 0.963$) and WST-D ($504 \pm 43 \mu\text{m}$ vs. $489 \pm 93 \mu\text{m}$, $p = 0.669$) impregnated samples. Similarly, within the patterned de-epithelialized subgroup, no difference in penetration depth was seen between channels and intermediate areas for both WST11 ($593 \pm 64 \mu\text{m}$ vs. $575 \pm 62 \mu\text{m}$, $p = 0.479$) and WST-D ($489 \pm 93 \mu\text{m}$ vs. $433 \pm 94 \mu\text{m}$, $p = 0.160$) impregnated samples. The addition of dextran significantly reduced the stromal penetration depth, in both fully and patterned de-epithelialized corneas, and in both channels and intermediate areas in patterned de-epithelialized corneas (both $p < 0.001$).

Efficacy

Strip extensiometry

Out of 120 corneas, three samples were excluded from analysis, due to testing apparatus failure (two samples) and as a result of sample slippage during testing (one sample). A significant CXL treatment effect ($p < 0.001$) was seen for all examined chromophores

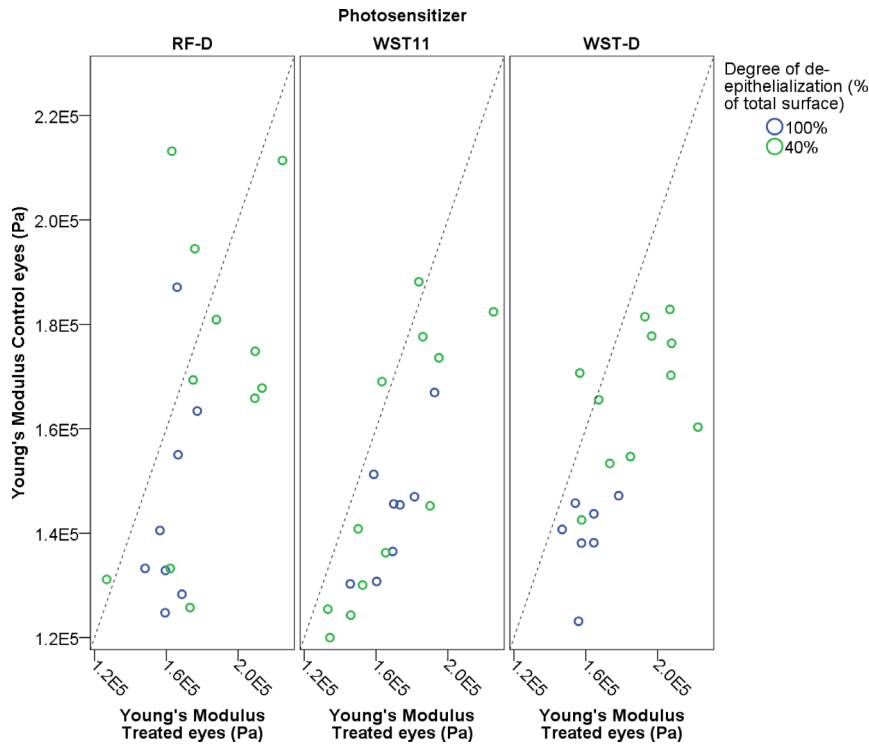


Fig. 7. Scatter plot of all paired corneal samples tested by strip extensimetry. Shown is the Young's Modulus of control samples (vertical axis) versus the Young's Modulus of its paired treated sample (horizontal axis), per chromophore and degree of epithelial removal (full, 100%; patterned, 40%). Treatment induced significant stiffening for all three chromophores ($p < 0.001$), without difference between chromophores ($p = 0.601$) or degree of epithelial removal ($p = 0.0564$). In Pascal, dashed line indicates equality between control and treated samples.

(RF-D, WST11 and WST-D). There was no difference in stiffening effect between chromophores ($p = 0.601$) or between fully or patterned de-epithelialized groups ($p = 0.564$). In the fully de-epithelialized samples, mean Young's Modulus for control versus treated corneas read 145.7 ± 21.4 kPa vs. 162.7 ± 8.8 kPa ($n = 8$), 144.2 ± 12.0 kPa vs. 168.9 ± 14.4 kPa ($n = 8$) and 139.5 ± 8.0 kPa vs. 160.3 ± 10.0 kPa ($n = 7$), for RF-D, WST11 and WST-D groups, respectively. Similarly, the respective means in the patterned de-epithelialized group were 169.8 ± 30.3 kPa vs. 183.7 ± 28.8 kPa ($n = 11$), 151.1 ± 25.3 kPa vs. 168.7 ± 27.8 kPa ($n = 12$) and 166.9 ± 12.9 kPa vs. 188.5 ± 22.3 kPa ($n = 11$). Figure 7 shows a scatter plot of all treated samples per chromophore and degree of de-epithelialization. Points to the upper left of the dashed line indicate no treatment effect was seen.

Discussion

As Wollensak's seminal publication, the Dresden CXL protocol, involving

central corneal epithelial removal, was first approved in Europe and recently in the United States (Wollensak, Spoerl & Seiler 2003). Keeping the epithelium intact during CXL could reduce pain and complications, such as delayed re-epithelialization, haze formation and microbial keratitis. It is, therefore, that many studies have focused on delivering RF to the corneal stroma without the removal of the epithelium, known as 'epi-on' CXL, by addition of penetration enhancers, alteration of the riboflavin formulation or by the use of iontophoresis (Beckman et al. 2019; Henriquez et al. 2020). Several studies show outcomes after epi-on treatment similar to the standard CXL procedures (Magli et al. 2013; Stojanovic, Zhou & Uthman 2014; Nawaz et al. 2015; Rossi et al. 2015; Stulting et al. 2018). However, similarly multiple studies do show inferior results after epi-on CXL (Wollensak & Iomdina 2009; Çerman, Toker & Ozarslan Ozcan 2015; Lombardo et al. 2015, 2019; Akbar et al. 2017; Godefrooij et al. 2017). The role of epithelial removal, therefore, remains subject of debate.

Several authors attempted to partially remove the corneal epithelium, either selectively leaving 'epithelial islands' in situ or by only removing superficial layers of the epithelium. While published data are limited, several clinical studies have been performed. Rechichi et al., Razmjoo et al., Hashemi et al. and Galvis et al. all manually removed only part of the epithelium, by repeatedly puncturing the epithelium with a self-made device, leaving the central 3 mm of epithelium in situ, or removing several parallel strips of epithelium, respectively (Rechichi et al. 2013; Razmjoo et al. 2014; Hashemi et al. 2015; Galvis et al. 2016). These studies not only show arrested progression and improved corrected distance visual acuity, but also indicate epi-off protocols provide superior improvement in topographic indices. Besides mechanical debridement, the application of alcohol (ALD) is now widely adopted, facilitating epithelial removal. While ALD was shown to result in a smoother surface, postoperative pain and epithelial healing time were shown to increase significantly (Katbab, Owji & Eghtedari 2012; Vingopoulos & Kanellopoulos 2019). In a recent study, Bradford et al. applied a femtosecond laser to create epithelial channels (Bradford et al. 2020). They show stromal RF concentrations of approximately 50% the concentration after regular epi-off protocols, but biomechanical effects are not reported on. While excimer lasers have been used to perform full epithelial debridement, to our knowledge, this is the first study to apply an excimer laser in order to create small epithelium penetrating channels (Kanellopoulos & Asimellis 2014; Sarac et al. 2018).

In corneal chromophore-based CXL, stromal chromophore distribution greatly determines the treatment's safety. For RF-based CXL, stromal RF is needed to sufficiently attenuate the applied toxic UVA light before reaching deeper ocular structures or inducing photochemical damage at the endothelial level (Wollensak et al. 2003; Marcovich et al. 2020). Thus, stromal RF concentration is an important measure in determining the treatment's safety. In standard epi-off CXL, this has been an area of great concern, specifically in thin corneas, and several solutions have been suggested, such as

covering the cornea with an additional layer of RF solution or by a RF soaked contact lens (Wollensak et al. 2010; Jacob et al. 2014; Hafezi et al. 2020). In WST11-based CXL, safe NIR light is applied, omitting the need to obtain sufficient stromal chromophore concentration to attenuate the applied light. For WST11-based CXL, chromophore penetration depth provides a more important safety measure, as a damaging photochemical reaction may still occur if WST11 reaches the endothelium. In this study, *total* transmission spectrometry was used to assess stromal chromophore concentrations, and confocal fluorescence microscopy allowed visualization of the chromophores' penetration depth. Lower stromal chromophore concentrations were seen by *total* transmission spectrometry in the patterned de-epithelialization group. Whereas RF was shown to penetrate the full stroma, regardless of Dextran addition or degree of de-epithelialization, confocal fluorescence microscopy showed that the addition of Dextran limits the stromal penetration depth of WST11 to the anterior half of the stroma. Thus, while for WST-D/NIR standard CXL parameters may be used safely in conjunction with this novel excimer laser-patterned de-epithelialization, protocol adaptation may be needed for RF/UVA CXL to ensure endothelial safety.

While this study provides a proof of concept, several limitations should be addressed. First, although we show that patterned de-epithelialization achieves similar stiffening as the regular Dresden protocol *ex vivo*, further *in vivo* models should address the clinical safety and efficacy. *Direct* transmission spectrometry shows increased scattering after patterned de-epithelialization, which indicates inferior optical clarity. This may be due to light absorption by remaining epithelium, the periodic structure of the laser ablation pattern or the irregular surface after excimer laser pretreatment (Pérez-Merino et al. 2010; Meek & Knupp 2015). Resolution of this increased scattering after epithelial healing could, however, not be confirmed in this *ex vivo* model. Also, while clinical studies suggest faster epithelial recovery and reduced post-operative pain after partial de-

epithelialization, this study cannot confirm or disprove these hypothesized benefits (Rechichi et al. 2013; Mazzotta & Ramovecchi 2014; Hashemi et al. 2015). Thus, future *in vivo* studies should investigate the technique's effect on corneal transparency and post-treatment epithelial healing and pain. Second, it is most likely corneal hydration *ex vivo* differs from the *in vivo* situation, with rapid swelling occurring after enucleation. As corneal swelling occurs mainly within the stroma, limited influence on excimer laser epithelial ablation may be expected, but stromal chromophore diffusion could differ from the *in vivo* situation. Third, in this study, an average epithelial thickness was determined for each cornea to set the laser's ablation depth, aimed to prevent ablation beyond the Bowman layer. In healthy eyes, this may be sufficient, as chromophore penetration may not be influenced by a thin layer of remaining epithelium due to only few tight junction complexes in the posterior epithelium, allowing a safe distance from the stroma (Bakke et al. 2009). However, in keratoconus eyes, the epithelium is known to be highly irregular and an average epithelial thickness would not suffice (Franco, White & Kruh 2020). In order to prevent stromal ablation, excimer laser-assisted patterned ablation of diseased eyes should thus involve accurate epithelial mapping with corresponding individualized and mapped ablation depth profiles. Given the fast-evolving imaging technology and increasing interest in personalized and targeted CXL, this limitation may soon be overcome. Last, while the total number of eyes in this study is high, the number of eyes per group as used for sub-analysis is relatively low.

In conclusion, the results of this study show the epithelium does not have to be removed completely to achieve effective corneal CXL but can be performed using an excimer laser to create epithelial channels, leaving approximately 60% of the epithelium in the treated area *in situ*. Stromal chromophore concentration, however, is found to be significantly lower when the epithelium is only partially removed and is influenced by the addition of Dextran. This raises safety implications for RF-based CXL, while less relevant for WST11-based CXL

due to its different safety mechanism. As interest in partial or selective de-epithelialization is growing along with customized cross-linking, and clinical studies applying partial mechanical de-epithelialization have already been partaken, these results may help to guide the development of a CXL technique reducing treatment burden, while guaranteeing patients' safety.

Acknowledgements

The authors would like to thank Amin Seraji from SCHWIND Eye-Tech-Solutions for his assistance during sample preparation, and Kathrin Benedikt and Udo Schmidt from Tomey GmbH for providing us with a CASIA2 ocular coherence tomographer during the experiments.

References

- Akbar B, Intisar-Ul-Haq R, Ishaq M, Fawad A, Arzoo S & Siddique K (2017): Comparison of transepithelial corneal crosslinking with epithelium-off crosslinking (epithelium-off CXL) in adult Pakistani population with progressive keratoconus. *Taiwan J Ophthalmol* 7: 185–190.
- Alageel SA, Arafat SN, Salvador-Culla B, Kolovou PE, Jahansair K, Kozak A, Braithwaite GJCC & Ciolino JB (2018): Corneal cross-linking with verteporfin and nonthermal laser therapy. *Cornea* 37: 362–368.
- Bakke EF, Stojanovic A, Chen X & Drolsum L (2009): Penetration of riboflavin and postoperative pain in corneal collagen crosslinking: excimer laser superficial versus mechanical full-thickness epithelial removal. *J Cataract Refract Surg* 35: 1363–1366.
- Beckman KA, Gupta PK, Farid M et al. (2019): Corneal crosslinking: Current protocols and clinical approach. *J Cataract Refract Surg* 45: 1670–1679.
- Bradford S, Mikula E, Xie Y, Juhasz T, Brown DJ & Jester JV (2020): Enhanced transepithelial riboflavin delivery using femtosecond laser-machined epithelial microchannels. *Transl Vis Sci Technol* 9: 1.
- Brekelmans J, Goz A, Dickman MM et al. (2017): Long-term biomechanical and histologic results of WST-D/NIR corneal stiffening in rabbits, up to 8 months follow-up. *Investig Ophthalmol Vis Sci* 58: 4089–4095.
- Cagil N, Sarac O, Cakmak HB, Can G & Can E (2015): Mechanical epithelial removal followed by corneal collagen crosslinking in progressive keratoconus: short-term complications. *J Cataract Refract Surg* 41: 1730–1737.
- Cerman E, Tokar E & Ozarslan Ozcan D (2015): Transepithelial versus epithelium-off crosslinking in adults with progressive keratoconus. *J Cataract Refract Surg* 41: 1416–1425.
- Cherfan D, Verter EE, Melki S et al. (2013): Collagen cross-linking using rose bengal and green light to increase corneal stiffness. *Investig Ophthalmol Vis Sci* 54: 3426–3433.
- Franco J, White CA & Kruh JN (2020): Analysis of compensatory corneal epithelial thickness changes in keratoconus using corneal tomography. *Cornea* 39: 298–302.

- Galvis V, Tello A, Carreño NI, Ortiz AI, Barrera R, Rodríguez CJ & Ochoa ME (2016): Corneal cross-linking (with a partial deepithelization) in keratoconus with five years of follow-up. *Ophthalmol Eye Dis* **8**: 17–21.
- Godefrooij DA, El KM, Soeters N & Wisse RP (2017): Higher order optical aberrations and visual acuity in a randomized controlled trial comparing transepithelial versus epithelium-off corneal crosslinking for progressive keratoconus. *Clin Ophthalmol* **11**: 1931–1936.
- Hafezi F, Kling S, Gilardoni F et al. (2020): Individualized corneal cross-linking with riboflavin and UV-A in ultra-thin corneas: the sub400 protocol. *Am J Ophthalmol*. **224**:133-142.
- Hashemi H, Mirafab M, Hafezi F & Asgari S (2015): Matched comparison study of total and partial epithelium removal in corneal cross-linking. *J Refract Surg* **31**: 110–115.
- Henriquez MA, Hernandez-Sahagun G, Camargo J & Izquierdo L (2020): Accelerated epi-on versus standard epi-off corneal collagen cross-linking for progressive keratoconus in pediatric patients: Five years of follow-up. *Cornea* **39**: 1493–1498.
- ICNIRP (International Commission on Non-ionizing Radiation Protection) (1997): Guidelines on limits of exposure to broad-band incoherent optical radiation (0.38 to 3 microM). International Commission on Non-Ionizing Radiation Protection. *Health Phys* **73**: 539–554.
- Jacob S, Kumar DA, Agarwal A, Basu S, Sinha P & Agarwal A. (2014): Contact lens-assisted collagen cross-linking (CACXL): A new technique for cross-linking thin corneas. *J Refract Surg* **30**: 366–372.
- Jay L, Brocas A, Singh K, Kieffer JC, Brunette I & Ozaki T (2008): Determination of porcine corneal layers with high spatial resolution by simultaneous second and third harmonic generation microscopy. *Opt Express* **16**(21): 16284–16293.
- Kanellopoulos AJ & Asimellis G (2014): Keratoconus management: long-term stability of topography-guided normalization combined with high-fluence CXL stabilization (the Athens Protocol). *J Refract Surg* **30**: 88–93.
- Katbab A, Owji SM & Eghtedari M (2012): Morphologic changes of corneal epithelial flap: Ethanol-mediated versus mechanical removal. *Ultrastruct Pathol* **36**: 400–403.
- Koller T, Mrochen M & Seiler T (2009): Complication and failure rates after corneal crosslinking. *J Cataract Refract Surg* **35**: 1358–1362.
- Lombardo M, Micali N, Villari V, Serrao S, Pucci G, Barberi R & Lombardo G (2015): Ultraviolet A: Visible spectral absorbance of the human cornea after transepithelial soaking with dextran-enriched and dextran-free riboflavin 0.1% ophthalmic solutions. *J Cataract Refract Surg* **41**: 2283–2290.
- Lombardo M, Serrao S, Lombardo G & Schiano-Lomoriello D (2019): Two-year outcomes of a randomized controlled trial of transepithelial corneal crosslinking with iontophoresis for keratoconus. *J Cataract Refract Surg* **45**: 992–1000.
- Magli A, Forte R, Tortori A, Capasso L, Marsico G & Piozzi E (2013): Epithelium-off corneal collagen cross-linking versus transepithelial cross-linking for pediatric keratoconus. *Cornea* **32**: 597–601.
- Maharana PK, Sahay P, Sujeeth M, Singhal D, Rath A, Titiyal JS & Sharma N (2018): Microbial keratitis after accelerated corneal collagen cross-linking in keratoconus. *Cornea* **37**: 162–167.
- Marcovich AL, Brandis A, Daphna O et al. (2012): Stiffening of rabbit corneas by the bacteriochlorophyll derivative WST11 using near infrared light. *Investig Ophthalmol Vis Sci* **53**: 6378–6388.
- Marcovich AL, Brekelmans J, Brandis A et al. (2020): Decreased riboflavin impregnation time does not increase the risk for endothelial phototoxicity during corneal cross-kinking. *Transl Vis Sci Technol* **9**: 4.
- Mazzotta Cosimo C & Ramovecchi V (2014): Customized epithelial debridement for thin ectatic corneas undergoing corneal cross-linking: Epithelial island cross-linking technique. *Clin Ophthalmol* **8**: 1337–1343.
- Meek KM & Knupp C (2015): Corneal structure and transparency. *Prog Retin Eye Res* **49**: 1–16.
- Nawaz S, Gupta S, Gogia V, Sasikala NK & Panda A (2015): Trans-epithelial versus conventional corneal collagen crosslinking: A randomized trial in keratoconus. *Oman J Ophthalmol* **8**: 9–13.
- Nibourg LM & Koopmans SA (2014): Preservation of enucleated porcine eyes for use in a wet laboratory. *J Cataract Refract Surg* **40**: 644–651.
- O’Brart DPS, Patel P, Lascaratos G, Wagh VK, Tam C, Lee J & O’Brart NA (2015): Corneal cross-linking to halt the progression of keratoconus and corneal ectasia: Seven-year follow-up. *Am J Ophthalmol* **160**: 1154–1163.
- Pérez-Merino P, Martínez-García MC, Mar-Sardaña S, Pérez-Escudero A, Blanco-Mezquita T, Mayo-Iscaar A & Merayo-Llves J (2010): Corneal light transmission and roughness after refractive surgery. *Optom Vis Sci* **87**: E469–E474.
- Poli M, Lefevre A, Auxenfans C & Burillon C (2015): Corneal collagen cross-linking for the treatment of progressive corneal ectasia: 6-year prospective outcome in a French population. *Am J Ophthalmol* **160**: 654–662e1.
- Raiskup F, Theuring A, Pillunat LE & Spoerl E (2015): Corneal collagen crosslinking with riboflavin and ultraviolet-A light in progressive keratoconus: Ten-year results. *J Cataract Refract Surg* **41**: 41–46.
- Peyman A, Kharraji M, Koosha N, Razmjoo H & Rahimi B. (2014): Corneal haze and visual outcome after collagen crosslinking for keratoconus: A comparison between total epithelium off and partial epithelial removal methods. *Adv Biomed Res* **3**: 221.
- Rechichi M, Daya S, Scorcio V, Meduri A & Scorcio G (2013): Epithelial-disruption collagen crosslinking for keratoconus: One-year results. *J Cataract Refract Surg* **39**: 1171–1178.
- Rossi S, Orrico A, Santamaria C, Romano V, De Rosa L, Simonelli F & De Rosa G (2015): Standard versus trans-epithelial collagen cross-linking in keratoconus patients suitable for standard collagen cross-linking. *Clin Ophthalmol* **9**: 503–509.
- Sarac O, Kosekahya P, Caglayan M, Tanriverdi B, Uzel AGT & Cagil N (2018): Mechanical versus transepithelial phototherapeutic keratectomy epithelial removal followed by accelerated corneal crosslinking for pediatric keratoconus: Long-term results. *J Cataract Refract Surg* **44**: 827–835.
- Stoddard JE, Marneris AG, Borr MJ & Keil ML (2018): Optimization of femtosecond lasers using porcine and human donor corneas before in vivo use. *J Cataract Refract Surg* **44**: 1018–1022.
- Stojanovic A, Zhou W & Utheim TP (2014): Corneal collagen cross-linking with and without epithelial removal: A contralateral study with 0.5% hypotonic riboflavin solution. *Biomed Res Int* **2014**:1–9. 619398.
- Stulting RD, Trattler WB, Woolfson JM & Rubinfeld RS (2018): Corneal crosslinking without epithelial removal. *J Cataract Refract Surg* **44**: 1363–1370.
- van de Kraats J & van Norren D (2007): Optical density of the aging human ocular media in the visible and the UV. *J Opt Soc Am A Opt Image Sci Vis* **24**: 1842–1857.
- Vingopoulos F & Kanellopoulos AJ (2019): Epibowman blunt keratectomy versus diluted EtOH epithelial removal in myopic photorefractive keratectomy: A prospective contralateral eye study. *Cornea* **38**: 612–616.
- Wollensak G, Aurich H, Wirbelauer C & Sel S (2010): Significance of the riboflavin film in corneal collagen crosslinking. *J Cataract Refract Surg* **36**: 114–120.
- Wollensak G & Iomdina E (2009): Biomechanical and histological changes after corneal crosslinking with and without epithelial debridement. *J Cataract Refract Surg* **35**: 540–546.
- Wollensak G, Spoerl E & Seiler T (2003): Riboflavin/ultraviolet-A-induced collagen crosslinking for the treatment of keratoconus. *Am J Ophthalmol, Behandlung von keratokonus durch kollagenvernetzung* **135**: 620–627.
- Wollensak G, Spoerl E, Wilsch M & Seiler T (2003): Endothelial cell damage after riboflavin-ultraviolet-A treatment in the rabbit. *J Cataract Refract Surg* **29**: 1786–1790.

Received on March 30th, 2021.
Accepted on August 31st, 2021.

Correspondence

Att. Jurriaan Brekelmans MD
University Eye Clinic Maastricht
Maastricht University Medical Center
P.O.B. 5800, 6202 AZ
Maastricht
The Netherlands
Phone: +31 43 387 1594
E-mail: jurriaan.brekelmans@mumc.nl

Conflict of Interest: J. Brekelmans, None; M.M. Dickman, None; S. Verma, SCHWIND Eye-Tech-Solutions (E); S. Arba-Mosquera, SCHWIND Eye-Tech-Solutions (E); R. Goldschmidt, None; A. Goz, None; A. Brandis, Steba Biotech (P); T.T.J.M. Berendschot, None; I.E.Y. Saelens, None; A.L. Marcovich, Steba Biotech (P), Yeda Weizmann (P), EyeYon Medical (C, P), Mor Isum (P); A. Scherz, Steba Biotech (C, P); R.M.M.A. Nuijts, Acufocus (S), Alcon (C, L, S), Asico (C), Bausch&Lomb (S), HumanOptics (S), Ophtec (S), ThéaPharma (C).

Funding: This work was supported by the Academic Incentive Fund azM/MUMC⁺ and the following foundations: Algemene Nederlandse Vereniging ter Voorkoming van Blindheid, Landelijke Stichting voor Blinden en Slechtzienden and Stichting Steunfonds Uitzicht that contributed through Uitzicht [grant number 2014-36]. The funding organizations provided unrestricted grants and had no role in the design or conduct of this research. AS is the inventor of WST-D licensed to Steba Biotech by ‘Yeda’ with royalties agreement. AB and AM are inventors of WST-D/NIR treatment with same.

Presented: Free paper abstract accepted to the 37th congress of the European Society of Cataract and Refractive Surgeons, Paris, France, September 2019 and to the CXL Experts’ Meeting, Zurich, Switzerland, December 2019.

Supporting Information

Additional Supporting Information may be found in the online version of this article:

- Fig S1
- Fig S2
- Table S1
- Equation S1